

# End-to-end Nanophotonics Inverse Design for Computational Imaging

Zin Lin<sup>1\*</sup>, Gaurav Arya<sup>1</sup>, William F. Li<sup>1</sup>, Charles Roques-Carmes<sup>2</sup>,  
Raphaël Pestourie<sup>1</sup>, Zhaoyi Li<sup>3</sup>, Federico Capasso<sup>3,4</sup>, Marin Soljačić<sup>2,4</sup> and  
Steven G. Johnson<sup>1</sup>

<sup>1</sup>Department of Mathematics, Massachusetts Institute of Technology, Cambridge MA 02138, USA

<sup>2</sup>Research Lab of Electronics, Massachusetts Institute of Technology, Cambridge MA 02138, USA

<sup>3</sup>John A. Paulson School of Engineering and Applied Sciences, Harvard University, Cambridge MA 02138, USA

<sup>4</sup>Department of Physics, Massachusetts Institute of Technology, Cambridge MA 02138, USA

\*zinlin@mit.edu

**Abstract:** We introduce end-to-end inverse design in which a nanophotonics frontend is optimized in conjunction with a computational-imaging backend to minimize reconstruction errors. We present several nanophotonics designs for depth, spectral and polarization imaging. © 2022 The Author(s)

Nanophotonics inverse design [1] enhances spatial, spectral and polarization sensitivities by leveraging full-wave Maxwell physics — electromagnetic interactions largely ignored by refractive or diffractive optics. Computational imaging transcends conventional optics by algorithmic reconstruction of high-fidelity information from limited optical measurements. We integrate nanophotonics inverse design and computational imaging into a holistic end-to-end [2] framework: a single-piece nanophotonics frontend is optimized in conjunction with an image-processing backend to minimize reconstruction errors. The optics and computation are tightly coupled because the gradient of the backend error is propagated through the entire pipeline to the physical parameters of the frontend nanophotonics. In contrast to optics-only or computation-only designs, the functionality of the frontend optics is not prescribed *a priori* but *spontaneously* emerges during the end-to-end optimization. Unfettered by human intervention, end-to-end discovery reveals nano-structures with enhanced data-acquisition capabilities and ultra-compact form factors.

Our end-to-end framework can be described in the most general term as the minimization of a loss function  $L(\tilde{\mathbf{u}}, \mathbf{u})$ , over geometrical parameters  $\varepsilon$  (belonging to the nanophotonics frontend) and hyperparameter(s)  $\alpha$  (belonging to the computational-imaging backend). Typically,  $L$  measures the distance between the (known) ground truth object  $\mathbf{u}$  and the reconstructed object  $\tilde{\mathbf{u}}$ . The latter is obtained by solving an inverse-scattering problem:

$$\tilde{\mathbf{u}} = \operatorname{argmin}_{\mu} \|\mathbf{G}\mu - \mathbf{v}\|^2 + R(\mu; \alpha), \quad (1)$$

where  $\mathbf{v}$  is a raw image,  $\mathbf{G}$  a measurement matrix, and  $R$  a regularization term. Note that the inverse-scattering problem (Eq. 1) is an *auxiliary* minimization problem “nested” within the *primary* problem of minimizing  $L$ . A key feature of our framework is an efficient differentiation of the *nested* minimization problem via an adjoint analysis of the associated Karush-Kuhn-Tucker optimality conditions. It is well known that Eq. 1 is typically ill-posed and an estimate  $\tilde{\mathbf{u}}$  may not be uniquely or stably determined. To facilitate the reconstruction, we incorporate additional *priors* (such as stability, smoothness and sparsity) in the form of  $R = \alpha\|\Psi\mu\|^2$  (Tikhonov regularization) or  $R = \alpha\|\Psi\mu\|_1$  (compressed sensing). Once  $R$  is specified,  $\tilde{\mathbf{u}}$  can be obtained by classical iterative algorithms with provable convergence and correctness. We note that, in contrast to data-driven approaches such as neural networks, our choice of classical methods to compute  $\tilde{\mathbf{u}}$  naturally prioritizes interpretability, generalizability and data-efficiency over learning deep data priors. Ultimately, future backends may be realized by new architectures that combine classical algorithms and deep neural networks.

In Eq. 1, the measurement matrix  $\mathbf{G}$  models the imaging optics and can be assembled from the electric field intensities on the CCD sensor in response to a point dipole at each position within the object space. In our image-formation models,  $\mathbf{G}$  can vary from convolutional kernels to full dense matrices. In fact, the richness and complexities of  $\mathbf{G}$  that arise from complex nanophotonics geometries and the underlying Maxwell equation differentiate our framework from refractive or diffractive optics. In particular, accurate computations of  $\mathbf{G}$  require detailed simulations of the nanophotonic geometry  $\varepsilon$  as well as the gradient  $\nabla_{\varepsilon}\mathbf{G}$  using the full Maxwell equation and its adjoint, taking into account strong spatio-spectral and polarization dispersions.

We present several examples to illustrate the capabilities of our framework. Figure 1a shows a large-area metasurface (an aperiodic nanophotonic structure made up of over one million subwavelength pillars) for single-shot multi-spectral imaging via Tikhonov-regularized reconstruction [3]. The metasurface is initialized as a uniform array of pillars with no prescribed functionality. As optimization progresses, a demultiplexing functionality emerges

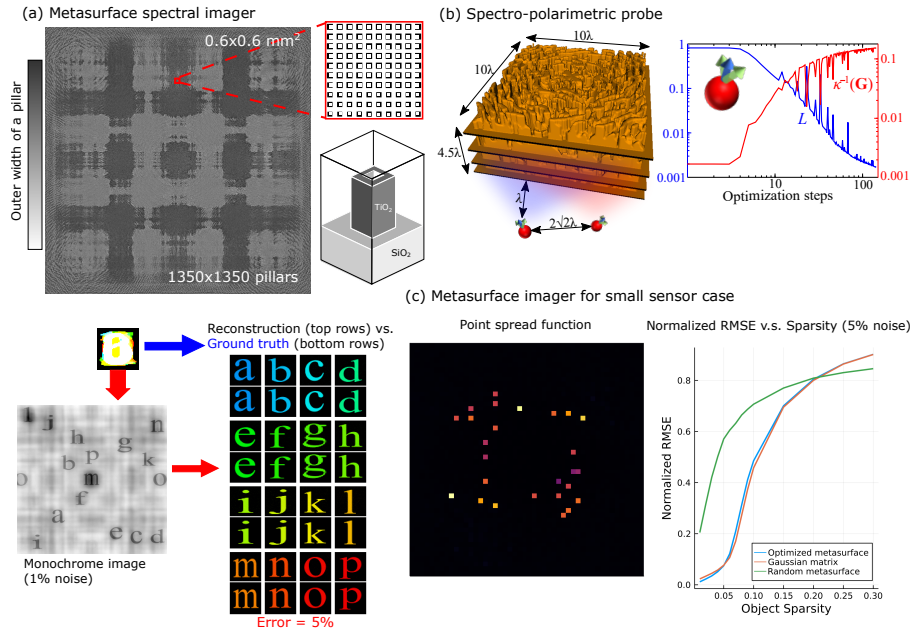


Fig. 1. (a) Metasurface spectral imager over the visible spectrum (450–660 nm). The test object is a multi-spectral image of superimposed letters, each letter emitting a different wavelength. The letters cannot be distinguished by naked eyes but are readily seen on the monochrome image and are accurately reconstructed by Tikhonov regularization. (b) Multi-layered polymer nanophotonic probe for sensing the polarization coherence states of fluorescence particles (up to two particles and two wavelengths). The loss function and the condition number  $\kappa(\mathbf{G})$  of the measurement matrix are simultaneously reduced as optimization progresses, rendering the final design  $\sim 100\times$  less prone to noise. (c) Metasurface 2D imager with compressed sensing (CS). The object has  $256 \times 256$  pixels and the sensor has  $128 \times 128$  pixels — an under-determined reconstruction problem. The end-to-end inverse design *spontaneously* configures a multi-focal metalens with 26 foci, which out-performs an un-optimized random metasurface while matching the “CS-optimal” performance of a (physically unrealistic) Gaussian matrix.

*spontaneously*, focusing the different spectral channels to separate domains on the monochrome sensor. Note that the locations of the domains do not follow any pre-determined pattern (such as an ordered lattice) but are optimally discovered by end-to-end inverse design. Figure 1b shows a topology-optimized volumetric nanophotonic probe for reconstructing the spatio-spectral polarization states of fluorescent particles up to two particles and two spectral bands [4]. We found that an end-to-end minimization of the Tikhonov-regularized reconstruction error simultaneously reduces the condition number  $\kappa(\mathbf{G})$  of the measurement matrix, enabling  $\sim 100\times$  reduction in noise sensitivity. Figure 1c shows the result of an end-to-end compressed-sensing (CS) optimization in the case of a “small sensor”. The reconstruction problem is under-determined, and the object is assumed to be sparse in the standard basis. The optimized design leads to  $\sim 10\times$  reduction in reconstruction errors compared to a random metasurface while it elegantly matches the performance of a “CS-optimal” but physically-unrealistic Gaussian matrix. Building on these examples, we will also present depth imagers, depth-spectral imagers and comprehensive spectro-polarimetric-depth imagers, each of which integrates an ultra-compact single-piece nanophotonics with an efficient Tikhonov and/or compressed-sensing backend without any additional optics.

## References

1. Sean Molesky, Zin Lin, Alexander Y Piggott, Weiliang Jin, Jelena Vucković, and Alejandro W Rodriguez. Inverse design in nanophotonics. *Nature Photonics*, 12(11):659, 2018.
2. Vincent Sitzmann, Steven Diamond, Yifan Peng, Xiong Dun, Stephen Boyd, Wolfgang Heidrich, Felix Heide, and Gordon Wetzstein. End-to-end optimization of optics and image processing for achromatic extended depth of field and super-resolution imaging. *ACM Transactions on Graphics (TOG)*, 37(4):1–13, 2018.
3. Zin Lin, Raphaël Pestourie, Charles Roques-Carmes, Zhaoyi Li, Federico Capasso, Marin Soljačić, Steven G Johnson. End-to-end metasurface inverse design for single-shot multi-channel imaging. *arXiv preprint arXiv:2111.01071*, 2021.
4. Zin Lin, Charles Roques-Carmes, Raphaël Pestourie, Marin Soljačić, Arka Majumdar, and Steven G Johnson. End-to-end nanophotonic inverse design for imaging and polarimetry. *Nanophotonics*, 10(3):1177–1187, 2021.